RESEARCH

Open Access

Biomechanical analysis of vertebral wedge deformity in elderly women with quantitative CT-based finite element analysis

Jing Liu[1], Xiaodong Cheng[2], Yan Wang[3], Ping Zhang[4], Lei Gao[4], Xingyuan Yang[1], Shaoqiang He[1], Ying Liu[4*†] and Wei Zhang[1*†]

Abstract

Background: To explore the vertebral deformity angle (VD angle) of 1st lumbar vertebral body (L1) in elderly women, investigate the influence of VD on vertebral stiffness (VS) by biomechanical analysis using quantitative computed tomography-based finite element analysis (QCT-FEA).

Methods: Two hundred seventy eight participants were recruited, and underwent QCT scan. Measured VD angles of L1, and constructed QCT-FEA models of L1 with the minimum (0.59°), median (5.79°) and maximum (11.15°) VD angles, respectively. Loads in two directions were applied on the upper edge of L1 with a force of 700 N, and vertebral stiffness (VS) was defined as the ratio of 700 N and displacement at the superior reference point: (1) perpendicular to the upper edge of L1 (defined as VS-U); (2) perpendicular to the lower edge of L1(defined as VS-L).

Results: Age was very weak positively correlated with VD angle, moderate negatively correlated with vBMD, and moderate negatively correlated with VS ($P < 0.05$). VS-U was significantly different among three VD angles, so was VS-L ($P < 0.001$). VS-U was higher than VS-L in 5.79° and 11.15° VD angles ($P < 0.05$), however no difference in 0.59° VD angles ($P > 0.10$).

Conclusions: VD angle of L1 was slightly increased with age and not correlated with vBMD, and VS was moderate negatively correlated with age, showing that the vertebral body was more likely to fracture with aging. VS-U and VS-L were gradually decreased with the increase of VD angle, and VS-L was lower than VS-U with the increase of VD angle, which showed that vertebral body was more prone to fracture when the load was perpendicular to the lower edge of the vertebral body as the VD angle increasing.

Keywords: Biomechanical analysis, Vertebral wedge deformity, Quantitative CT, Finite element analysis

†Ying Liu and Wei Zhang contributed equally to this work.

*Correspondence: 18503117687@163.com; dreamflytir@163.com; zw77988@163.com

[1] Department of Radiology, The Third Hospital of Hebei Medical University, No. 139 Ziqiang St, Qiaoxi District, Shijiazhuang, Hebei CN 050050, China
[4] Department of CT/MRI, The Third Hospital of Hebei Medical University, No. 139 Ziqiang St, Qiaoxi District, Shijiazhuang, Hebei CN 050050, China
Full list of author information is available at the end of the article

Background

Vertebral deformity (VD) is mainly attributable to osteoporosis and classical hallmark of osteoporosis, associated with marked increase in morbidity, mortality and health economic burden [1]. There are three types of VD, crush, wedge and biconcave, of which the most common type is controversial [2–4]. Some studies showed that wedge deformity is the most frequent and tends to cluster at the mid-thoracic and thoracolumbar regions of the spine [2, 5–7], while some studies suggested that biconcavity is

Liu *et al. BMC Musculoskeletal Disorders* (2022) 23:575

Page 2 of 8

the most common type [8, 9]. VD is increased with age and more marked in women [2], because there is often no remembered injury and visible fracture plane on radiographs [1, 10], and the term "deformity" is often used rather than "fracture" [11]. Previous studies suggest that gradual time-dependent "creep" processes may contribute to VD, which is continuing deformation under constant load [10, 12, 13]. Some studies regarding restoration of vertebral height had been reported [14–16]. However, few studies focus on the influence of VD on vertebral stiffness (VS).

Quantitative computed tomography (QCT) has become the most common tool for measuring volume bone mineral density (vBMD), which can avoid the influence of vertebral osteophyte, facet degeneration, intervertebral disc stenosis, endplate sclerosis and abdominal aortic wall calcification [17–19]. However, given the fact that fracture is a biomechanical phenomenon by its nature, bone mineral density (BMD) may not be the most effective tool for fracture risk assessment [20]. QCT-based finite element analysis (QCT-FEA) promises an improved tool for assessing fracture-related mechanical characteristics (e.g.: stiffness and strength) on patient-specific basis accounting for BMD [21–24].

The purpose of our study was to explore the vertebral deformity angle (VD angle) of 1st lumbar vertebral body (L1) in elderly women, and investigate the influence of VD angle on VS by biomechanical analysis using QCT-FEA.

Methods

Patient population

We retrospectively reviewed a single-center database of QCT examination from January 2017 to December 2019 with approval from the local institutional review board (2018–036-1). Written informed consent was provided to all participants before QCT examination. Inclusion criteria: women from 50 to 80 years old and underwent MRI examination within one week interval from QCT to exclude L1 vertebral compression fracture. Exclusion criteria: vertebral fracture and/or surgery, and biconcave or crush deformity of L1. Age, height and weight were recorded, and height and weight were measured by standard method. Body mass index (BMI) was defined as weight (kg) divided by height squared (m^2).

Image acquisition

All participants underwent cross-sectional CT scan of L1 (from the 12th thoracic to 2nd lumbar vertebra) in the supine position by using CT scanner (Somatom Sensation 64, Siemens, Erlangen, Germany) with hands above the head and a solid Mindways QCT phantom (Mindways Software Inc., Austin, TX, USA) closely dorsal side of each participant simultaneously. CT scan was performed using the following parameters: 120 kV, 125 mAs, 168 cm table height, 512×512 matrix, 1 mm slice thickness, and 500 mm field of view.

Image analysis

VD angle

The measurement method of VD angle was shown in Fig. 1, and VD angles were measured by two analysts (a primary analyst, Y.L., with 5 years of imaging diagnostic experience, and a secondary analyst, J. L., with 3 years of imaging diagnostic experience), and then took their average for further used. VD angles of 278 participants were not normal distribution, and we constructed QCT-FEA models of L1 with the minimum (0.59°), median (5.79°) and maximum (11.15°) VD angles, respectively (Fig. 2).
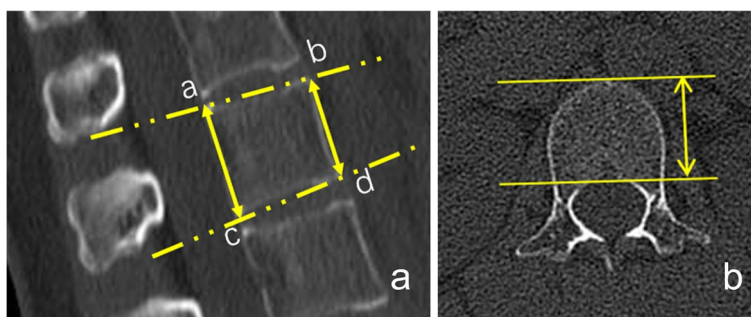

Fig. 1 Schematic diagram of VD angle measurement of L1. **a**: Four marginal points (a, b, c and d) of the maximum sagittal plane of the L1 vertebral body were established, and distance between point a and point **c** (identified D_{ac}), and distance between point **b** and point **d** (identified D_{bd}) were measured. **b**: The tangent line of the anterior arc at the maximum plane of the axial L1 vertebral body was identified as the anterior edge line, and the parallel line of the anterior edge line and across the posterior margin of the vertebral body was identified as the posterior edge line. Distance between the anterior edge line and the posterior edge line was identified D_{ap}. VD angle = (D_{ac}—D_{bd})/ D_{ap}. VD angle: vertebral deformity angle. L1: 1st lumbar vertebral body

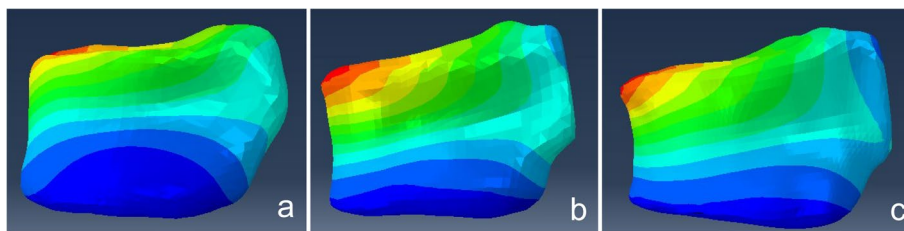Liu *et al. BMC Musculoskeletal Disorders*   (2022) 23:575

Page 3 of 8

Fig. 2 QCT-FEA models with three different VD angles of L1. **a**: QCT-FEA model with VD angle of 0.59 degrees. **b**: QCT-FEA model with VD angle of 5.79 degrees. **c**: QCT-FEA model with VD angle of 11.15 degrees. QCT-FEA: quantitative computed tomography-based finite element analysis. VD angle: vertebral deformity angle. L1: 1st lumbar vertebral body

vBMD

Images were transferred to a QCT workstation and analyzed using the three-dimensional spine function version 5.10 of Mindways QCT pro soft-ware (Mindways Software Inc., Austin, TX, USA). Regions of interest (ROI) about 250 mm^2 area and 9 mm height was placed at the midplane of L1 vertebral body to avoid the influence of cortical bone and proliferative osteophyte. vBMD were measured by two radiologists, and then took the average for analysis.

QCT-FEA models

We constructed QCT-FEA models of L1 using the Mimics program (Mimics 21.0, Materialize Inc, Leuven, Belgium) and Geomagic Studio 2013 (Geomagic, Inc., Research Triangle Park, NC, USA). Three-dimensional finite element models were built by converting each voxel in the QCT images directly into a linear cube-shaped tetrahedral element. QCT images of DICOM format were imported into Mimics, vertebral bone was segmented out, and then coronal, sagittal and axial images of lumbar vertebra were obtained. Threshold, split mask, edit masks, calculate three dimensions and other steps were performed of L1 to fill the holes and remove the sharp angles, and then a preliminary three-dimensional geometric model was obtained. The preliminary three-dimensional geometric model was imported into Geomagic Studio of STL format, smoothened, and then exported into STP/STEP format. The spine structure is complex, so in this study, the vertebral body accessory, intervertebral disc, ligament muscle and other structures were removed, and only the vertebral body was analyzed for the need to simplify the models. In Abaqus software, material properties of L1 were endowed. The material property (e.g., elastic modulus) of each element was automatically mapped from the corresponding voxel of the CT dataset based on its Hounsfield unit (HU) [25, 26]. The relationship between HU and QCT-measured BMD (ρQCT, mg/cm^3) has been assumed linear [27, 28], and was determined based on the calibration phantoms:

$$\rho QCT = 0.5325 Hu - 38.401$$

An empirical relationship between BMD and elastic modulus (E, MPa), which was previously established based on mechanical testing of the human vertebral cadavers, was used to determine the material properties of the bone elements [29, 30]:

$$E = 4730 \rho QCT^{1.56}$$

The Poisson's ratio was set to 0.3, as commonly used in bone QCT-based finite element models [22, 31].

Biomechanical analysis

Abaqus software (Abaqus 6.13, Dassault Systèmes, RI, USA) was used for biomechanical analysis of three angles QCT-based finite element model among each participant, respectively. The boundary was set, and freedom of all nodes on the lower surface of L1 was set to 0. Loads in two directions were applied on the upper edge of L1 with a force of 700 N centrally:(1) perpendicular to the upper edge of L1; (2) perpendicular to the lower edge of L1 (Fig. 3).

Previous study showed that the force of 700 N represented approximately the upper limit of the linear portion of the load–displacement curve derived from all vertebral specimens in vitro cadaver experiment, and VS was defined as the ratio of the applied force (700 N) and its resulted displacement at the superior reference point [22]. VS when the load perpendicular to the upper edge of L1 was defined as VS-U, and the load perpendicular to the lower edge of L1 was defined as VS-L.

Statistical analysis

Statistical analyses were performed using SPSS version 26.0. Shapiro–Wilk (SW) test was used to test whether the data accorded with normal distribution, and $P < 0.05$ was considered significant. Statistical description of the quantitative variables was expressed
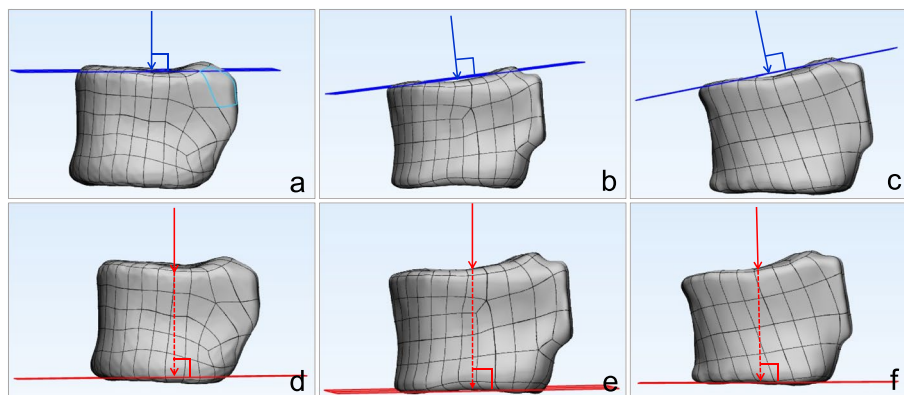
Liu *et al. BMC Musculoskeletal Disorders*   (2022) 23:575

Page 4 of 8

Fig. 3 Schematic diagram of different directional loads applied on the QCT-FEA models. **a** and **d**: QCT-FEA model with VD angle of 0.59 degrees. **b** and **e**: QCT-FEA model with VD angle of 5.79 degrees. **c** and **f**: QCT-FEA model with VD angle of 11.15 degrees. **a**, **b** and **c**: Loads perpendicular to the upper edge of L1 were applied to the upper edge of L1 with a force of 700 N. **d**, **e** and **f**: Loads perpendicular to the lower edge of L1 were applied to the upper edge of L1 with a force of 700 N. QCT-FEA: quantitative computed tomography-based finite element analysis. VD angle: vertebral deformity angle. L1: 1st lumbar vertebral body

as mean $\pm$ standard deviation (SD) or median (P$_{25}$, P$_{75}$). Pearson or spearman correlation test was used to test the correlation among age, BMI, VD angle, vBMD and VS, and $P < 0.05$ was considered significant. Kruskal–Wallis H test was used to test the difference of VS-U among three VD angles ($P < 0.05$ was considered significant), and then Mann–Whitney U test for pairwise comparison, and statistical test criteria for pairwise comparison was calibrated as α'=α/3, that was 0.05/3. Statistical analysis method of VS-L is the same as that of VU-U. Two independent Mann–Whitney U test was used to compare the difference between VS-U and VS-L of the same VD angle, and $P < 0.05$ was considered significant.

Results

Descriptive statistics and correlation analysis

Two hundred seventy eight female participants were included (Table 1).

Age was not correlated with BMI ($r = -0.012$, $P = 0.842$), very weak positively correlated with VD angle ($r = 0.191$, $P = 0.001$), moderate negatively correlated with vBMD ($r_s = -0.481$, $P < 0.001$), and moderate negatively correlated with VS (r_s raged from -0.479 to -0.481, P all < 0.001).

BMI was not correlated with VD angle ($r = -0.018$, $P = 0.762$), not correlated with vBMD ($r_s = 0.093$, $P = 0.121$), and not correlated with VS (r_s raged from 0.092 to 0.097, P all > 0.05).

VD angle was not correlated with vBMD ($r_s = -0.017$, $P = 0.778$), and not correlated with VS (r_s raged from -0.017 to -0.018, P all > 0.05).

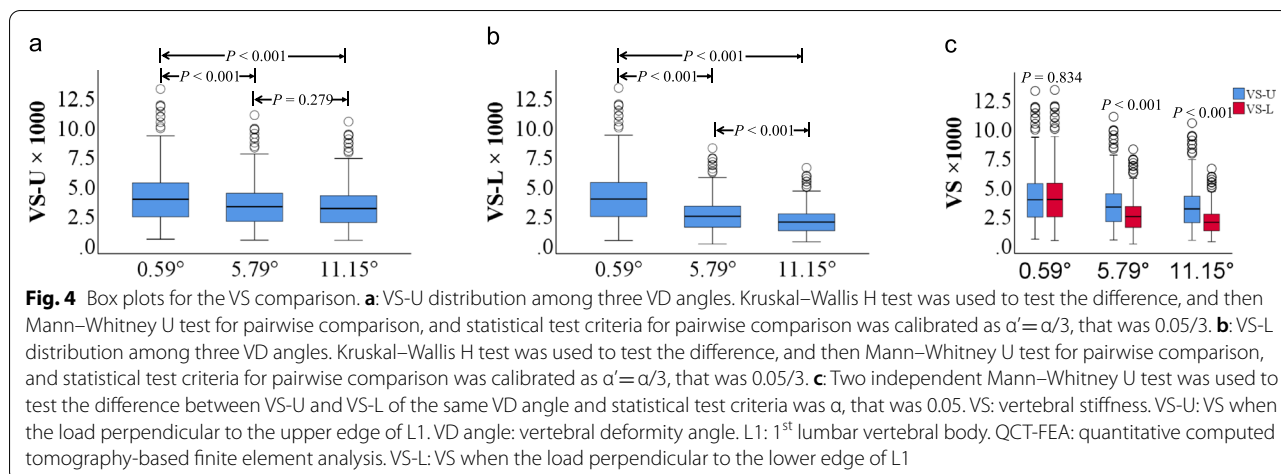**Table 1** Descriptive characteristics of the female participants

	All participants
n	278
Age (years)	63.8 ± 8.4
BMI (Kg/m^2)	25.3 ± 3.7
vBMD(mg/cm^3)	94.1(68.5, 114.9)
VD angle	5.74 ± 1.91
QCT-FEA model with VD angle of 0.59 degrees	
VS-U	3838.8(2337.8, 5240.5)
VS-L	3864.2(2353.3, 5273.1)
QCT-FEA model with VD angle of 5.79 degrees	
VS-U	3198.5(1948.0, 4365.5)
VS-L	2378.9(1436.9, 3246.4)
QCT-FEA model with VD angle of 11.15 degrees	
VS-U	3038.2(1850.1, 4145.7)
VS-L	1892.7(1152.7, 2582.8)

Note: *BMI* Body mass index, *vBMD* Volume bone mineral density, *VD angle* Vertebral deformity angle of L1, *QCT-FEA* Quantitative computed tomography-based finite element analysis, *VS-U* Vertebral stiffness when the load perpendicular to the upper edge of 1st lumbar vertebral body, *VS-L* Vertebral stiffness when the load perpendicular to the lower edge of 1st lumbar vertebral body

Comparison of VS

VS-U was significantly different among three VD angles ($Z = 556.000$, $P < 0.001$), and then for pairwise comparison, there were difference between 0.59° and 5.79°, between 0.59° and 11.15°, and no difference between 5.79° and 11.15° VD angles (Fig. 4a).

VS-L was significantly different among three VD angles ($Z = 548.029$, $P < 0.001$), and then for pairwise comparison, there were difference between 0.59° and 5.79°,

Liu *et al. BMC Musculoskeletal Disorders*   (2022) 23:575

Page 5 of 8

Fig. 4 Box plots for the VS comparison. **a**: VS-U distribution among three VD angles. Kruskal–Wallis H test was used to test the difference, and then Mann–Whitney U test for pairwise comparison, and statistical test criteria for pairwise comparison was calibrated as α'=α/3, that was 0.05/3. **b**: VS-L distribution among three VD angles. Kruskal–Wallis H test was used to test the difference, and then Mann–Whitney U test for pairwise comparison, and statistical test criteria for pairwise comparison was calibrated as α'=α/3, that was 0.05/3. **c**: Two independent Mann–Whitney U test was used to test the difference between VS-U and VS-L of the same VD angle and statistical test criteria was α, that was 0.05. VS: vertebral stiffness. VS-U: VS when the load perpendicular to the upper edge of L1. VD angle: vertebral deformity angle. L1: 1st lumbar vertebral body. QCT-FEA: quantitative computed tomography-based finite element analysis. VS-L: VS when the load perpendicular to the lower edge of L1

between 0.59° and 11.15°, and between 5.79° and 11.15° VD angles (Fig. 4b).

VS-U was higher than VS-L in 5.79° and 11.15° VD angles ($P < 0.05$), however no difference in 0.59° VD angles ($P > 0.10$, Fig. 4c).

Discussion

Present study showed that age was very weak positively correlated with VD angle, consistent with previous study, which showed that VD was increased with age and was more marked in women [2]. Age was moderate negatively correlated with vBMD, and the loss of BMD in women consists of two stages, slow constant age-related loss and quick oestrogen-dependent process, which begins after the menopause. Hormonal imbalance, ageing, environmental factors, life style, and genetic predispositions are responsible for about 50–80% of BMD loss [32]. Previous studies showed that typical anterior wedge deformity can be created consistently in cadaveric vertebrae in a 2-stage process. First, compressive overload fractures the endplate, decompresses the adjacent intervertebral disc, and concentrates loading onto the anterior cortex. Second, cyclic loading in flexion causes progressive collapse of the anterior cortex [11]. In our study, VD angle was not correlated with vBMD. This may be pseudomorph that increased vBMD caused by trabecular insertion of microfracture after vertebral wedge deformity, or the fact that vertebral wedge deformity mainly involves bone density under the endplate of the vertebral body, while QCT measures the vBMD of cancellous bone in the center of the vertebral body, without zonal measurement of BMD. Previous study showed that trabecular density is lower in the anterior versus posterior regions of the vertebral centrum [33], micro trabecular fractures and endplate fractures are commonly seen in osteoporotic vertebral bodies, and often in vertebrae that appeared to be uninvolved on specimen radiographs [34].

The density-modulus relationship was directly adopted from a previous study where mechanical testing was conducted on vertebral bone of white subjects; thus, the predictive abilities of our QCT-FEA models for stiffness are well validated [22, 29, 30]. VS was defined as the ratio of the applied force (700 N) and its resulted displacement at the superior reference point, reflecting the ability of vertebral body to resist fracture to some extent. In present study, VS was moderate negatively correlated with age, showing that the vertebral body was more likely to fracture with aging. VS-U and VS-L were all significantly different among three VD angles, and decreased as the VD angle increases. In present study, as the VD angle increasing, VS-U was different from VS-L, and VS-U was higher than VS-L, which showed that vertebral body was more prone to fracture when the load was perpendicular to the lower edge of the vertebral body as the VD angle increasing. This may be due to the fact that the angle between the upper edge of L1 and the Y-axis line is usually greater than the angle between the lower edge of L1 and the Y-axis line after the vertebral wedge deformity (as shown in Fig. 5, angle α usually greater than angle β). Why is angle α usually greater than angle β, the reason may be that, from the perspective of biomechanical analysis, the force on the upper edge of the vertebral body should be consistent with the lower edge, however, when the force on the lower edge may be buffered when it comes into contact with structures like the disc reducing the reaction force, so the deformation degree of the upper edge was slightly heavier. Thus, as shown in Fig. 5, the load a is equal to the b, the force leading to the anterior and posterior displacement of the vertebral body in the Y-axis direction is small and can be ignored, and the Z-axis component force of load b is greater than load a
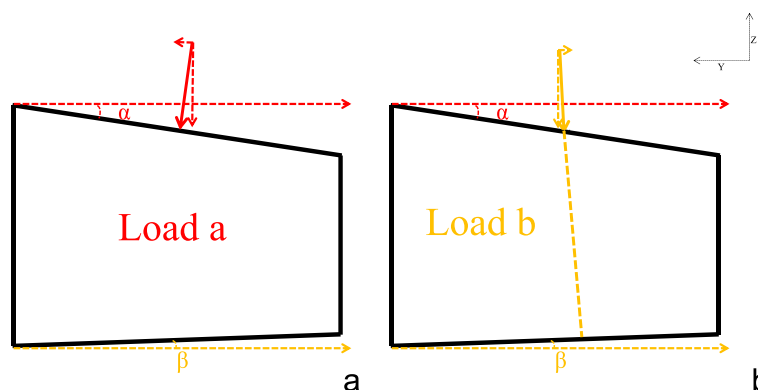
Liu *et al. BMC Musculoskeletal Disorders*   (2022) 23:575

Page 6 of 8

Fig. 5 Schematic diagram of L1 vertebral body anterior wedge deformity of sagittal plane. Y axis and Z axis are the human coordinate system. **a**: Load a (solid red line with arrow) perpendicular to the upper edge of L1 was applied to the upper edge of L1 with a force of 700 N. **b**: Load b (solid yellow line with arrow) perpendicular to the lower edge of L1 was applied to the upper edge of L1 with a force of 700 N. The angle between the upper edge of L1 and Y axis was defined as angle α. The angle between the lower edge of L1 and Y axis was defined as angle β. L1: 1st lumbar vertebral body

because of angle α greater than angle β. Thus, when load b is applied, the displacement of L1 is larger and the VS is smaller. Or this may be pseudomorph caused by the removal of vertebral body accessory, intervertebral disc, ligament muscle and other structures.

Several limitations should be discussed. Firstly, the vertebral body accessory, intervertebral disc, ligament muscle and other structures were removed, and only the vertebral body was analyzed for QCT-FEA models. Secondly, only three VD angles of QCT-FEA models were reconstructed. While now, FEA of each patient's clinical-resolution computed tomography scan, accounting for variations in geometry, cortical thickness, and material properties to assess bone stiffness and bone strength [35], is now available in the USA as a Medicare screening benefit for osteoporosis diagnostic testing, helping to address under-diagnosis of osteoporosis [21]. However, the process is complicated and time-consuming. We focused on the influence of VD on VS, so simplified the model and only three different VD angles were analyzed. Thirdly, only loads in two directions and only VS were analyzed in QCT-FEA, experimental results had not been verified in vivo, and only VS was analyzed without vertebral strength or follow-up of fracture probability. Experimental stiffness of the whole vertebral body was measured as the slope of the linear portion of the load–displacement curve, i.e., between 26 and 56% of the peak force, and experimental strength of the vertebral body was defined as the peak force at the load–displacement curve [22]. Through previous studies, the vertebral stiffness has a formula consistent with the results of the carcass analysis, and can also reflect the state of vertebral body [22].

Finally, this was a single-center study and the sample size of 70–80 years is slightly smaller.

Conclusions

We demonstrated that VD angle of L1 was slightly increased with age and not correlated with vBMD, and VS was moderate negatively correlated with age, showing that the vertebral body was more likely to fracture with aging. VS-U and VS-L were gradually decreased with the increase of VD angle, and VS-L was lower than VS-U with the increase of VD angle, which showed that vertebral body was more prone to fracture when the load was perpendicular to the lower edge of the vertebral body as the VD angle increasing.

Supplementary information

The online version contains supplementary material available at https://doi.org/10.1186/s12891-022-05518-z.

Additional file 1.

Liu *et al. BMC Musculoskeletal Disorders*   (2022) 23:575

Page 7 of 8

Declarations

Ethics approval and Consent to participate

All methods were approved by the ethics committee of the Third Hospital of Hebei Medical University (reference numbers: 2018–036-1) and was performed in accordance with the Declaration of Helsinki. Informed consent was obtained from all patients for this study, all patients agreed to participate in the study.

Consent for publication

Not applicable.

Competing interests

The authors declare that there is no conflict of competing financial and non-financial interests.

Author details

[1]Department of Radiology, The Third Hospital of Hebei Medical University, No. 139 Ziqiang St, Qiaoxi District, Shijiazhuang, Hebei CN 050050, China. [2]Key Laboratory of Biomechanics of Hebei Province and Orthopaedic Research Institution of Hebei Province, Shijiazhuang 050000, Hebei, China. [3]Department of Endocrinology, The Third Hospital of Hebei Medical University, No. 139 Ziqiang St, Qiaoxi District, Shijiazhaung, Hebei CN 050000, China. [4]Department of CT/MRI, The Third Hospital of Hebei Medical University, No. 139 Ziqiang St, Qiaoxi District, Shijiazhuang, Hebei CN 050050, China.

References

1. Morosano ME, Menoyo I, Caferra DA, Sánchez A, Tomat MF, Bocanera R, Pezzotto SM, Masoni AM. Vulnerability of healthy vertebrae in patients with and without previous vertebral fracture. Bone. 2011;48:820–7. https://doi.org/10.1016/j.bone.2010.12.014.
2. Ismail AA, Cooper C, Felsenberg D, Varlow J, Kanis JA, Silman AJ, O'Neill TW. Number and type of vertebral deformities: epidemiological characteristics and relation to back pain and height loss. European Vertebral Osteoporosis Study Group. Osteoporos Int. 1999;9(3):206–13.
3. Ma C, Wu F, Pan F F, Laslett L, Shah A, Squibb K, Winzenberg T, Jones G. Bone Microarchitecture, Volumetric or Areal Bone Mineral Density for Discrimination of Vertebral Deformity in Adults: A Cross-sectional Study. J Clin Densitom. 2021;24(2):190–9.
4. Genant HK, Wu CY, van Kuijk C, Nevitt MC: Vertebral fracture assessment using a semiquantitative technique. Journal of bone and mineral research : the official journal of the American Society for Bone and Mineral Research 1993, 8:1137–1148.https://doi.org/10.1002/jbmr.5650080915.
5. Eastell R, Cedel SL, Wahner HW, Riggs BL, Melton LJ, 3rd: Classification of vertebral fractures. Journal of bone and mineral research : the official journal of the American Society for Bone and Mineral Research 1991, 6:207–215.https://doi.org/10.1002/jbmr.5650060302.
6. Mann T, Oviatt SK, Wilson D, Nelson D, Orwoll ES: Vertebral deformity in men. Journal of bone and mineral research : the official journal of the American Society for Bone and Mineral Research 1992, 7:1259–1265.https://doi.org/10.1002/jbmr.5650071120.
7. Melton LJ 3rd, Kan SH, Frye MA, Wahner HW, O'Fallon WM, Riggs BL. Epidemiology of vertebral fractures in women. Am J epidemiol. 1989;129(5):1000–11.
8. Wáng YXJ, Lentle BC. Radiographic osteoporotic vertebral fractures in elderly men: a brief review focusing on differences between the sexes. Quant imaging med surg. 2020;10(9):1863–76.
9. Lunt M, O'Neill TW, Felsenberg D, Reeve J, Kanis JA, Cooper C, Silman AJ. Characteristics of a prevalent vertebral deformity predict subsequent vertebral fracture: results from the European Prospective Osteoporosis Study (EPOS). Bone. 2003;33(4):505–13.
10. Pollintine P, Luo J, Offa-Jones B, Dolan P, Adams MA. Bone creep can cause progressive vertebral deformity. Bone. 2009;45(3):466–72.
11. Landham PR, Gilbert SJ, Baker-Rand HL, Pollintine P, Robson Brown KA, Adams MA, Dolan P. Pathogenesis of Vertebral Anterior Wedge Deformity: A 2-Stage Process? Spine. 2015;40:902–8.
12. Haagensen CD, Stout AP. Synovial Sarcoma. Ann surg. 1944;120(6)::826-842.
13. Luo J, Pollintine P, Gomm E, Dolan P, Adams MA: Vertebral deformity arising from an accelerated "creep" mechanism. European spine journal : official publication of the European Spine Society, the European Spinal Deformity Society, and the European Section of the Cervical Spine Research Society 2012, 21:1684–1691.https://doi.org/10.1007/s00586-012-2279-y.
14. Zhao WT, Qin DP, Zhang XG, Wang ZP, Tong Z. Biomechanical effects of different vertebral heights after augmentation of osteoporotic vertebral compression fracture: a three-dimensional finite element analysis. J orthop surg res. 2018;13:32.
15. Jacobson RE, Nenov A, Duong HD. Re-expansion of Osteoporotic Compression Fractures Using Bilateral SpineJack Implants: Early Clinical Experience and Biomechanical Considerations. Cureus. 2019;11:e4572.
16. Ottardi C, La Barbera L, Pietrograde L, Villa T. Vertebroplasty and kyphoplasty for the treatment of thoracic fractures in osteoporotic patients: a finite element comparative analysis. J appl biomater funct mat. 2016;14:e197-204.
17. Li N, Li XM, Xu L, Sun WJ, Cheng XG, Tian W. Comparison of QCT and DXA: Osteoporosis Detection Rates in Postmenopausal Women. Int J endocrinol. 2013;2013:895474.
18. Khoo BC, Brown K, Cann C, Zhu K, Henzell S, Low V, Gustafsson S, Price RI, Prince RL. Comparison of QCT-derived and DXA-derived areal bone mineral density and T scores. Osteoporos Int. 2009;20:1539–45.
19. Zhang W, Ma X, Xue P, Gao Y, Wu X, Zhao J, Wang Y, Li S. Associations between fat distribution and volumetric bone mineral density in Chinese adults. Endocrine. 2014;47:862–8.
20. Kanis JA, Johnell O, Oden A, Johansson H, McCloskey E. FRAX and the assessment of fracture probability in men and women from the UK. Osteoporos Int. 2008;19:385–97.
21. Keaveny TM, Clarke BL, Cosman F, Orwoll ES, Siris ES, Khosla S, Bouxsein ML. Biomechanical Computed Tomography analysis (BCT) for clinical assessment of osteoporosis. Osteoporos Int. 2020;31:1025–48.
22. Wei Y, Feng W, Li G, Li Z, Liu Z, Cheng X, Yang H. Experimental testing and biomechanical CT analysis of Chinese cadaveric vertebrae with different modeling approaches. Med eng phys. 2021;93:8–16.
23. Suzuki T, Matsuura Y, Yamazaki T, Akasaka T, Ozone E, Matsuyama Y, et al. Biomechanics of callus in the bone healing process, determined by specimen-specific finite element analysis. Bone 2020;132:115212.
24. Allaire BT, Lu D, Johannesdottir F, Kopperdahl D, Keaveny TM, Jarraya M, et al. Prediction of incident vertebral fracture using CT-based finite element analysis. Osteoporos Int. 2019;30::323-331.
25. Crawford RP, Cann CE, Keaveny TM. Finite element models predict in vitro vertebral body compressive strength better than quantitative computed tomography. Bone 2003;33:744–50.
26. Zeinali A, Hashemi B, Akhlaghpoor S: Noninvasive prediction of vertebral body compressive strength using nonlinear finite element method and an image based technique. Physica medica : PM : an international journal devoted to the applications of physics to medicine and biology : official journal of the Italian Association of Biomedical Physics (AIFB) 2010, 26:88–97.https://doi.org/10.1016/j.ejmp.2009.08.002.

Liu *et al. BMC Musculoskeletal Disorders*   (2022) 23:575

Page 8 of 8

27. Buckley JM, Loo K, Motherway J. Comparison of quantitative computed tomography-based measures in predicting vertebral compressive strength. Bone. 2007;40:767–74.
28. Crawford RP, Rosenberg WS, Keaveny TM. Quantitative computed tomography-based finite element models of the human lumbar vertebral body: effect of element size on stiffness, damage, and fracture strength predictions. J biomech eng. 2003;125:434–8.
29. Giambini H, Dragomir-Daescu D, Nassr A, Yaszemski MJ, Zhao C. Quantitative Computed Tomography Protocols Affect Material Mapping and Quantitative Computed Tomography-Based Finite-Element Analysis Predicted Stiffness. J biomech eng. 2016;138:0910031–7.
30. Morgan EF, Bayraktar HH, Keaveny TM. Trabecular bone modulus-density relationships depend on anatomic site. J biomech. 2003;36:897–904.
31. Schileo E, Balistreri L, Grassi L, Cristofolini L, Taddei F. To what extent can linear finite element models of human femora predict failure under stance and fall loading configurations. J biomech. 2014;47:3531–8.
32. Syed FA, Ng AC. The pathophysiology of the aging skeleton. Curr Osteoporos Rep. 2010;8:235–40.
33. Oda K, Shibayama Y, Abe M, Onomura T. Morphogenesis of vertebral deformities in involutional osteoporosis. Age-related, three-dimensional trabecular structure. Spine. 1998;23:1050–5 discussion 1056.
34. Antonacci MD, Mody DR, Rutz K, Weilbaecher D, Heggeness MH. A histologic study of fractured human vertebral bodies. J spinal disord tech. 2002;15:118–26.
35. Costa MC, Eltes P, Lazary A, Varga PP, Viceconti M, Dall'Ara E. Biomechanical assessment of vertebrae with lytic metastases with subject-specific finite element models. J mech behav biomed mater. 2019;98:268–90.

Publisher's note